

*Hawaii Geothermal Project*

THE  
**HAWAII GEOTHERMAL  
PROJECT**

FREE CONVECTION ABOUT A VERTICAL  
CYLINDER EMBEDDED IN A POROUS MEDIUM

TECHNICAL REPORT No. 11



FREE CONVECTION ABOUT A VERTICAL  
CYLINDER EMBEDDED IN A POROUS MEDIUM

TECHNICAL REPORT No. 11

November 5, 1975

Prepared Under

NATIONAL SCIENCE FOUNDATION  
Research Grant No. GI-38319

and

ENERGY RESEARCH AND DEVELOPMENT ADMINISTRATION  
Research Grant No. E(04-3)-1093

By

W. J. Minkowycz\*  
Department of Energy Engineering  
University of Illinois at Chicago Circle  
Chicago, Illinois

and

Ping Cheng\*\*  
Department of Mechanical Engineering  
University of Hawaii  
Honolulu, Hawaii

---

\*Associate Professor  
\*\*Professor

## NOMENCLATURE

A	constant defined by Eq. (6b)
C	constant defined by Eq. (58)
$C_1$	constant defined by Eq. (31c)
$C_p$	specific heat of the convective fluid
$D_1$	constant given by Eq. (31d)
$D_3$	constant given by Eq. (41c)
F	transformed stream function defined by Eq. (17)
G	auxiliary function defined by Eq. (32a)
g	acceleration of gravity
K	permeability of the porous medium
$k_m$	thermal conductivity of the porous medium
L	length of the cylinder
$P_1$	quantity defined by Eq. (31a)
$P_2$	quantity defined by Eq. (40a)
$P_3$	quantity defined by Eq. (41a)
p	pressure
Q	surface - integrated heat transfer rate
$Q_1$	quantity defined by Eq. (31b)
$Q_2$	quantity defined by Eq. (40b)
$Q_3$	quantity defined by Eq. (41b)
q	local heat transfer rate per unit area
$Ra_x$	modified local Rayleigh number, $Ra_x \equiv K\rho_\infty g\beta x(T_w - T_\infty)/\mu\alpha$
r	radial coordinate
$r_0$	radius of cylinder

S	spanwise dimension, $S = 2\pi r_0$
T	temperature
u	velocity component in x-direction
$u_r$	reference velocity, $u_r \equiv K\rho_\infty g\beta(T_w - T_\infty)/\mu$
v	reference velocity in r-direction
x	axial coordinate
$\alpha$	equivalent thermal diffusivity
$\beta$	coefficient of thermal expansion
$\eta$	pseudo-similarity variable defined by Eq. (15)
$\theta$	dimensionless temperature defined by Eq. (18)
$\lambda$	constant defined by Eq. (6b)
$\mu$	viscosity of convective fluid
$\rho$	density of convective fluid
$\xi$	stretched streamwise coordinate defined by Eq. (16)
$\xi_0$	constant defined by $\xi_0 \equiv (2/r_0) \sqrt{\frac{\mu\alpha}{K\rho_\infty\beta gA}}$
$\xi_L$	constant defined by $\xi_L = (2/r_0) \sqrt{\frac{\mu\alpha L}{K\rho_\infty\beta g(T_w - T_\infty)_L}}$
$\phi$	auxiliary function defined by Eq. (32b)
$\psi$	stream function

### Subscripts

c	quantities associated with a cylinder
p	quantities associated with a flat plate
w	quantities on the surface of the cylinder
$\infty$	quantities at infinity

## LIST OF FIGURES

1. Dimensionless temperature and vertical velocity profiles: (a)  $\lambda = 0$ , (b)  $\lambda = 1/2$ , and (c)  $\lambda = 1$
2. Local heat transfer ratio for selected values of  $\lambda$
3. Total heat transfer ratio for any  $\lambda$

## ABSTRACT

An analysis is made for free convective flow about a vertical cylinder embedded in a saturated porous medium, where surface temperature of the cylinder varies as  $x^\lambda$ , a power function of distance from the leading edge. Within the framework of boundary layer approximations, exact solution is obtained for the special case where surface temperature varies linearly with  $x$ , i.e.,  $\lambda = 1$ . For other values of  $\lambda$ , approximate solutions based on local similarity and local non-similarity models are obtained. It is found that the local similarity solutions are sufficiently accurate for all practical purposes. Analytical expressions for local surface heat flux and overall surface heat flux are obtained.

## 1. INTRODUCTION

The study of free convection from the outer surface of a heated vertical cylinder embedded in a saturated porous medium has important geophysical and engineering applications. For example, as a result of volcanic activities or tectonic movements, magmatic intrusion may occur at shallow depths in the earth's crust [1]. The intrusive magma may take the form of a cylindrical shape. If the intrusive magma is trapped in an aquifer, free convective flow can be generated in the groundwater adjacent to the hot intrusives. A study of temperature distribution around the intrusives and the associated heat flux distribution will aid in an assessment and the evaluation of geothermal resources during geophysical exploration. Furthermore, the heat transfer coefficients obtained from this study will be useful to estimate the cooling rate of intrusive bodies and consequently the life span of a geothermal reservoir; it will also be useful to calculate the heat loss of underground casing and piping systems for the optimum design of geothermal power plants.

It has been established that a viable geothermal reservoir for power generation must have a hot heat source for the continuous supply of energy, and a highly permeable formation to ensure sustained delivery of fluids to production wells at adequate rates [2]. Under these conditions, free convective flow in geothermal reservoirs will have a high Rayleigh number. Accordingly, boundary layer approximations, analogous to the classical viscous theory, can be applied to free convective flow in a porous medium. This has been done by Wooding [3] to treat the problem of free convection about a line source and a point source, as well as for free convection above two finite heated vertical plates embedded in a porous medium. The boundary layer approximations were also invoked by McNabb [4] to treat the problem of free convective flow in a porous medium above a horizontal heated plate.

Most recently, Cheng and his co-workers [5,6] have obtained similarity solutions for free convection in a porous medium adjacent to vertical and horizontal plates with wall temperatures being a power function of distance.

In this paper we shall study convective flow about a vertical heated cylinder embedded in a saturated porous medium, where surface temperature of the cylinder varies as  $x^\lambda$ , a power function of distance from the leading edge. Within the framework of boundary layer approximations, exact solution is obtained for the special case where surface temperature varies linearly with  $x$ , i.e.,  $\lambda = 1$ . For other values of  $\lambda$ , approximate solutions based on local similarity and local non-similarity methods [7,8] are obtained. It is found that the local similarity solutions are sufficiently accurate for all practical purposes.

## 2. FORMULATION OF THE PROBLEM

Consider the problem of steady free convection about a vertical cylinder of radius  $r_0$ , with a prescribed axial symmetric wall temperature, is embedded in a saturated porous medium as shown in Fig. 1. If we assume that 1) the convective fluid and the porous medium are everywhere in local thermodynamic equilibrium, 2) the temperature of the fluid is everywhere below boiling, 3) properties of the fluid and the porous medium is everywhere isotropic and homogeneous, and 4) Boussinesq approximation is employed, the governing equations in a cylindrical coordinate system are given by

$$\frac{\partial}{\partial r}(rv) + \frac{\partial}{\partial x}(ru) = 0 \quad , \quad (1)$$

$$u = -\frac{K}{\mu} \left( \frac{\partial p}{\partial x} + \rho g \right) \quad , \quad (2)$$



$$v = -\frac{K}{\mu} \frac{\partial p}{\partial r} , \quad (3)$$

$$u \frac{\partial T}{\partial x} + v \frac{\partial T}{\partial r} = \alpha \left[ \frac{1}{r} \frac{\partial}{\partial r} \left( r \frac{\partial T}{\partial r} \right) + \frac{\partial^2 T}{\partial x^2} \right] , \quad (4)$$

$$\rho = \rho_{\infty} \left[ 1 - \beta(T - T_{\infty}) \right] , \quad (5)$$

where  $u$ , and  $v$  are the velocity components in  $x$  and  $r$ -directions,  $\rho$ ,  $\mu$ , and  $\beta$  are the density, viscosity, and the thermal expansion coefficient of the fluid,  $K$  is the permeability of the saturated porous medium,  $\alpha = k_m / (\rho C_p)_f$  is the equivalent thermal diffusivity where  $k_m$  denoting the thermal conductivity of the saturated porous medium and  $(\rho C_p)_f$  the density and specific heat of the fluid.  $T$ ,  $p$ , and  $g$  are respectively the temperature, pressure, and the gravitational acceleration. The subscript " $\infty$ " denotes the condition at infinity. The appropriate boundary conditions for the problem are

$$r = r_0 , \quad v = 0 , \quad T = T_w = T_{\infty} + Ax^{\lambda} , \quad (6a,b)$$

$$r \rightarrow \infty , \quad u = 0 , \quad T = T_{\infty} , \quad (7a,b)$$

where  $A > 0$ . In Eq. (6b) we have assumed that the prescribed wall temperature is a power function of distance from the leading edge.

The continuity equation is automatically satisfied by introducing the stream function  $\psi$  as

$$ru = \frac{\partial \psi}{\partial r} \quad \text{and} \quad rv = -\frac{\partial \psi}{\partial x} . \quad (8)$$

The governing equations and boundary conditions in terms of  $\psi$  and  $T$  are given by

$$\frac{\partial}{\partial r} \left( r \frac{\partial \psi}{\partial r} \right) + \frac{1}{r} \frac{\partial^2 \psi}{\partial x^2} = \frac{\rho_{\infty} \beta K g}{\mu} \frac{\partial T}{\partial r} \quad , \quad (9)$$

$$\frac{\partial \psi}{\partial r} \frac{\partial T}{\partial x} - \frac{\partial \psi}{\partial x} \frac{\partial T}{\partial r} = \alpha \left[ \frac{\partial}{\partial r} \left( r \frac{\partial T}{\partial r} \right) + r \frac{\partial^2 T}{\partial x^2} \right] \quad , \quad (10)$$

and

$$r = r_0 \quad , \quad \frac{\partial \psi}{\partial x} = 0 \quad , \quad (11)$$

$$r \rightarrow \infty \quad , \quad \frac{\partial \psi}{\partial r} = 0 \quad , \quad (12)$$

with the remaining two boundary conditions for T being given by Eqs. (6b) and (7b).

### 3. BOUNDARY LAYER EQUATIONS

The boundary layer approximations similar to those by Wooding [3], McNabb [4], Cheng & Minkowycz [5], and Cheng & Chang [6] can now be applied if we assume that convection takes place within a thin layer adjacent to the vertical surface of the cylinder. With these simplifications, Eqs. (9) and (10) become

$$\frac{\partial}{\partial r} \left( \frac{1}{r} \frac{\partial \psi}{\partial r} \right) = \frac{\rho_{\infty} \beta g K}{\mu} \frac{\partial T}{\partial r} \quad , \quad (13)$$

and

$$\alpha \frac{\partial}{\partial r} \left( r \frac{\partial T}{\partial r} \right) = \left( \frac{\partial \psi}{\partial r} \frac{\partial T}{\partial x} - \frac{\partial \psi}{\partial x} \frac{\partial T}{\partial r} \right) \quad . \quad (14)$$

We now attempt to transform Eqs. (13) and (14) into a set of ordinary differential equations. For this purpose we introduce the following new dimensionless variables

$$\eta = \sqrt{\frac{K \rho_{\infty} g \beta (T_w - T_{\infty})}{\mu \alpha x}} \left[ \frac{r_0}{2} \left( \frac{r^2}{r_0^2} - 1 \right) \right] = \sqrt{\frac{Ra_x}{x}} \left[ \frac{r_0}{2} \left( \frac{r^2}{r_0^2} - 1 \right) \right] \quad , \quad (15)$$

$$\xi = \frac{2}{r_0} \sqrt{\frac{\mu \alpha x}{K \rho_{\infty} \beta g (T_w - T_{\infty})}} = \frac{2x}{r_0} \frac{1}{\sqrt{Ra_x}} \quad , \quad (16)$$

where  $Ra_x \equiv K\rho_\infty g\beta(T_w - T_\infty)/\mu\alpha$  is the modified local Rayleigh number in a saturated porous medium. It is worth mentioning that for a thin boundary layer where  $r$  does not differ appreciably from  $r_0$ , the quantity inside the bracket in Eq. (15) reduces to  $y$  (where  $y = r - r_0$ ) and consequently  $\eta$  reduces to the flat plate similarity variable given in Ref. 5. Next we introduce the dimensionless stream function and temperature  $F$  and  $\theta$  given by

$$\psi = r_0 \sqrt{\frac{\alpha K \rho_\infty g \beta (T_w - T_\infty) x}{\mu}} F(\xi, \eta) = \alpha r_0 \sqrt{Ra_x} F(\xi, \eta) \quad , \quad (17)$$

$$\theta(\xi, \eta) = \frac{T - T_\infty}{T_w - T_\infty} \quad , \quad (18)$$

which are identical to the relations for a flat plate [5] except that  $F$  is now a function of both  $\xi$  and  $\eta$  and  $r_0$  is introduced to give proper dimension for  $\psi$ .

It can be shown that velocity components in terms of the new variables are

$$u = \frac{K\rho_\infty g(T_w - T_\infty)}{\mu} F_\eta \quad , \quad (19)$$

and

$$v = \frac{r_0}{2r} \sqrt{\frac{\alpha K \rho_\infty g \beta (T_w - T_\infty)}{\mu x}} \left[ (1-\lambda)(\eta F_\eta - \xi F_\xi) - (1+\lambda)F \right] \quad , \quad (20)$$

whereas the governing equations (13) and (14) with appropriate boundary conditions in terms of the new variables are

$$F_{\eta\eta} = \theta_\eta \quad , \quad (21)$$

$$\frac{\partial}{\partial \eta} \left[ (1+\xi\eta) \frac{\partial \theta}{\partial \eta} \right] + \frac{(1+\lambda)}{2} F_{\theta\eta} - \lambda F_\eta \theta = \frac{1-\lambda}{2} \xi (F_\eta \theta_\xi - \theta_\eta F_\xi) \quad , \quad (22)$$

$$F(\xi, 0) = 0 \quad , \quad \theta(\xi, 0) = 1 \quad , \quad (23a,b)$$

$$F'(\xi, \infty) = 0, \quad \theta(\xi, \infty) = 0 \quad (24a,b)$$

It is worth noting that Eqs. (21) and (22) are identical to those for free convection about a vertical flat plate [5] if  $\xi = 0$ . Thus, any deviation from  $\xi = 0$  is a measure of transverse curvature effects. We shall now obtain approximate solutions for  $\lambda \neq 1$  and exact solutions for  $\lambda = 1$ .

#### 4. APPROXIMATE SOLUTIONS FOR $\lambda \neq 1$

##### A. Local Similarity Solution

When the value of  $\xi$  or the values of  $\theta_\xi$  and  $F_\xi$  are both small, the right-hand side of Eq. (22) can be deleted. With this approximation, Eqs. (21-24) do not have derivatives with respect to  $\xi$  and thus can be considered as a coupled pair of ordinary differential equations with  $\xi$  regarded as a prescribed parameter. This is the so-called local similarity approximation. Thus, the local similarity equations are given by

$$F'' = \theta' \quad (25)$$

and

$$(1 + \xi\eta)\theta'' + \left(\xi + \frac{1+\lambda}{2}F\right)\theta' - \lambda F'\theta = 0 \quad (26)$$

with boundary conditions given by

$$F(\xi, 0) = 0, \quad \theta(\xi, 0) = 1 \quad (27a,b)$$

$$F'(\xi, \infty) = 0, \quad \theta(\xi, \infty) = 0 \quad (28a,b)$$

where the primes denote partial differentiation with respect to  $\eta$ .

We now obtain numerical solution to Eqs. (25) and (26) by an integral method. To this end, we first integrate Eq. (25) and impose condition (27a) and (27b) to give

$$F(\xi, \eta) = \int_0^\eta \theta(\xi, \eta) d\eta \quad (29)$$

We now turn our attention to Eq. (26) which can be considered as a second-order ordinary differential equation for  $\theta$ . The solution for  $\theta$  is given by

$$\theta(\xi, \eta) = \int_0^\eta \left[ \int_0^\eta Q_1(\xi, \eta) e^{\int_0^\eta P_1(\xi, \eta) d\eta} + C_1 \right] e^{-\int_0^\eta P_1(\xi, \eta) d\eta} d\eta + D_1, \quad (30)$$

$$\text{where } P_1(\xi, \eta) \equiv \left[ \xi + \frac{1+\lambda}{2} F(\xi, \eta) \right] / (1+\xi\eta), \quad (31a)$$

$$Q_1(\xi, \eta) \equiv \frac{\lambda F' \theta}{1+\xi\eta} = \frac{\lambda \theta^2}{1+\xi\eta}, \quad (31b)$$

$$C_1 \equiv - \frac{D_1 + \int_0^\infty \left[ e^{-\int_0^\eta P_1 d\eta} \int_0^\eta Q_1 e^{\int_0^\eta P_1 d\eta} d\eta \right] d\eta}{\int_0^\infty e^{-\int_0^\eta P_1 d\eta} d\eta}, \quad (31c)$$

and

$$D_1 = 1, \quad (31d)$$

with constants (31c) and (31d) obtained by imposing Eq. (30) with boundary conditions (27) and (28).

By assigning a successive value of  $\xi$  and assuming initial profile for  $\theta$ , values of stream function and temperature at a particular location  $(\xi, \eta)$  can be obtained by iteration from the integrals given by Eqs. (29) and (30). The solution thus obtained is an approximate one since some terms in the energy equation are assumed to be small.

#### B. Local Non-Similarity Solution

More accurate results can be obtained by the so-called local non-similarity solution which retains the full energy equation. To this end, we let

$$G(\xi, \eta) \equiv \frac{\partial F}{\partial \xi}, \quad (32a)$$

$$\phi(\xi, \eta) \equiv \frac{\partial \theta}{\partial \xi} \quad , \quad (32b)$$

and Eqs. (21) and (22) can be rewritten as

$$F'' = \theta' \quad , \quad (33)$$

$$(1+\xi\eta)\theta'' + \left(\xi + \frac{1+\lambda}{2}F + \frac{1-\lambda}{2}\xi G\right)\theta' = \lambda F'\theta + \frac{1-\lambda}{2}\xi F'\phi \quad . \quad (34)$$

It is noted that Eqs. (33) and (34) do not have derivatives with respect to  $\xi$ . However, we now have four unknowns and therefore two more equations are needed. For this purpose, we differentiate Eqs. (33) and (34) with respect to  $\xi$  to give

$$G'' = \phi' \quad , \quad (35)$$

$$(1+\xi\eta)\phi'' + \left(\xi + \frac{1+\lambda}{2}F\right)\phi' = \left(\frac{1+\lambda}{2}\right)F'\phi + \lambda G'\theta - (1+G)\theta' - \eta\theta'' + \frac{1-\lambda}{2}\xi \frac{\partial}{\partial \xi}(F'\phi - \theta'G) \quad , \quad (36)$$

where we have made use of Eq. (32).

If the last term of Eq. (36) vanishes, Eqs. (33-36) can be considered as a set of coupled ordinary differential equations with  $\xi$  regarded as a parameter. The last term is vanishing small if either  $\xi$  or  $\frac{\partial}{\partial \xi}(F'\phi - \theta'G)$  is small.

If the last term in Eq. (36) is deleted, we have

$$(1+\xi\eta)\phi'' + \left(\xi + \frac{1+\lambda}{2}F\right)\phi' = \left(\frac{1+\lambda}{2}\right)F'\phi + \lambda G'\theta - (1+G)\theta' - \eta\theta'' \quad . \quad (37)$$

Eqs. (33), (34), (35), and (37) are referred to as the first level of truncation of a local non-similarity model, which can be considered as four coupled ordinary differential equations for  $F$ ,  $\theta$ ,  $G$ , and  $\phi$  with  $\xi$  regarded as a parameter. These equations are to be solved subject to the following boundary conditions

$$F(\xi,0) = 0 , \quad \theta(\xi,0) = 1 , \quad (38a)$$

$$F'(\xi,\infty) = 0 , \quad \theta(\xi,\infty) = 0 , \quad (38b)$$

$$G(\xi,0) = 0 , \quad \phi(\xi,0) = 0 , \quad (38c)$$

$$G'(\xi,\infty) = 0 , \quad \phi(\xi,\infty) = 0 . \quad (38d)$$

Thus the local non-similarity solution retains the full energy equation with approximations made in a subsidiary equation, and therefore, the local non-similarity solution is expected to be more accurate than the local similarity solution.

Numerical solution to the local non-similarity equations can also be obtained by the integral method described previously for the local similarity solution. Integrating Eqs. (33) and (35) we have

$$F(\xi,\eta) = \int_0^\eta \theta(\xi,\eta') d\eta' , \quad (39a)$$

$$G(\xi,\eta) = \int_0^\eta \phi(\xi,\eta') d\eta' . \quad (39b)$$

The solution to Eq. (34) is identical to Eq. (30) in form, but with  $P_1$  and  $Q_1$  replaced by  $P_2$  and  $Q_2$  where

$$P_2(\xi,\eta) = \left( \xi + \frac{1+\lambda}{2} F + \frac{1-\lambda}{2} \xi G \right) / (1+\xi\eta) , \quad (40a)$$

$$Q_2(\xi,\eta) = \left( \lambda F' \theta + \frac{1-\lambda}{2} \xi F' \phi \right) / (1+\xi\eta) . \quad (40b)$$

Similarly, the solution to Eq. (37) is also given by Eq. (30), but with  $P_1$ ,  $Q_1$ , and  $D_1$  replaced by  $P_3$ ,  $Q_3$ , and  $D_3$  where

$$P_3(\xi, \eta) = \left( \xi + \frac{1+\lambda}{2} F \right) / (1+\xi\eta) \quad , \quad (41a)$$

$$Q_3(\xi, \eta) = \left[ \frac{1+\lambda}{2} F' \phi + \lambda G' \theta + (1+G)\theta' - \eta(Q_2 - P_2\theta') \right] / (1+\xi\eta) \quad , \quad (41b)$$

$$D_3 = 0 \quad . \quad (41c)$$

By assigning a value for  $\xi$  and with an initial guess of  $\theta$  and  $\phi$ , solutions to  $F$ ,  $G$ ,  $\theta$ , and  $\phi$  can be obtained by iteration.

Presumably, more accurate results can be obtained by introducing subsidiary equations from successive differentiation of the energy equation and deleting the terms involving  $\xi$  derivatives in the last subsidiary equation. From the previous work by Sparrow and Yu [7] and by Minkowycz and Sparrow [8], it is shown that the first level of truncation of the local non-similarity solution is sufficiently accurate, and therefore, higher level of truncations have not been pursued in this paper.

##### 5. EXACT SOLUTION FOR $\lambda = 1$

It is interesting to note that exact solution for Eqs. (13) and (14) are possible if wall temperature varies linearly with height. For the special case of  $\lambda = 1$ , Eqs. (15-18) are given by

$$\eta = \sqrt{\frac{K\rho_\infty g\beta A}{\mu\alpha}} \left[ \frac{r_0}{2} \left( \frac{r^2}{r_0^2} - 1 \right) \right] \quad , \quad (42)$$

$$\xi_0 = \frac{2}{r_0} \sqrt{\frac{\mu\alpha}{K\rho_\infty g\beta A}} \quad , \quad (43)$$

$$\psi = r_0 \sqrt{\frac{\alpha K\rho_\infty g\beta A}{\mu}} x F(\eta) \quad , \quad (44)$$

$$\theta(\eta) \equiv \frac{T - T_\infty}{Ax} \quad , \quad (45)$$



where both  $\eta$  and  $\xi_0$  are independent of  $x$  with  $\eta$  depending only on  $r$  and  $\xi_0$  is a constant. Furthermore, for  $\lambda = 1$ , the right-hand side of Eq. (22) vanishes exactly. Thus Eqs. (21) and (22) become

$$F_{\eta\eta} = \theta_{\eta} \quad , \quad (46)$$

$$\frac{\partial}{\partial \eta} \left[ (1 + \xi_0 \eta) \frac{\partial \theta}{\partial \eta} \right] + F \theta_{\eta} - F_{\eta} \theta = 0 \quad , \quad (47)$$

$$F(0) = 0 \quad , \quad \theta(0) = 1 \quad , \quad (48)$$

$$F'(\infty) = 0 \quad , \quad \theta(\infty) = 0 \quad . \quad (49)$$

Eqs. (46-49) are identical to Eqs. (25-28) with  $\lambda = 1$  and  $\xi = \xi_0$ . Thus the solutions to the local similarity solution is an exact one for  $\lambda = 1$ , and is an approximate one for  $\lambda \neq 1$ .

## 6. RESULTS AND DISCUSSION

Computations for local similarity solutions given by Eqs. (25-28) as well as the first level truncation of the local non-similarity solutions given by Eqs. (33-35) and Eqs. (37-38) are carried out for  $\lambda = 0, 1/4, 1/3, 1/2$  and  $3/4$ . Exact numerical solution given by Eqs. (46-49) for  $\lambda = 1$  are also obtained for the range of  $\xi_0$  from 0 to 20. According to Eq. (21) and Eq. (24), the values of  $\theta$  and  $F'$  (where  $F' = u/u_r$  and  $u_r \equiv \rho_{\infty} g \beta K (T_w - T_{\infty}) / \mu$ ) are the same for any  $\eta$ . Thus these values are plotted as the vertical coordinate in Fig. 1. The difference in values between the local similarity solution and the local non-similarity solution is too small to be plotted in the figures. It is shown in these figures that both the dimensionless temperature and vertical velocity have a maximum value of 1 at  $\eta = 0$ ; their values decrease as  $\eta$  is increased. The boundary layer thickness is shown to be increasing when either

$\lambda$  is decreased or  $\xi$  is increased. The magnitude of temperature gradient at the wall, i.e.,  $[-\theta'(\xi,0,\lambda)]$ , is shown to be increasing as  $\xi$  or  $\lambda$  is increased. The variation of  $[-\theta'(\xi,0,\lambda)]$  with respect to  $\xi$  and  $\lambda$  are also tabulated in Table 1.

The local surface heat flux can be computed from

$$q_c = -k_m \left( \frac{\partial T}{\partial r} \right)_{r=r_0} , \quad (50)$$

which can be expressed in terms of dimensionless variables to give

$$q_c(x) = k_m A^{3/2} \sqrt{\frac{\rho_\infty g \beta K}{\mu \alpha}} x^{\frac{3\lambda-1}{2}} [-\theta'(\xi,0,\lambda)] , \quad (51)$$

where it should be noted that  $\xi = \xi_0$  for  $\lambda = 1$ . Eq. (51) is identical to the corresponding expression for free convection about a vertical flat plate [5] if the quantities  $[-\theta'(\xi,0,\lambda)]$  is replaced by  $[-\theta'(0,\lambda)]$ . It follows, therefore, the ratio of the surface heat flux along a vertical cylinder to that of a flat plate embedded in the same porous medium and with the same wall temperature variation is given by

$$\frac{q_c(x)}{q_p(x)} = \frac{[-\theta'(\xi,0,\lambda)]}{[-\theta'(0,\lambda)]} , \quad (52)$$

where the subscripts "c" and "p" are used to denote the quantities associated with a cylinder and a flat plate respectively. Numerical results for Eq. (52) based on both local similarity solution and local non-similarity solution are tabulated in Table 2 and are also plotted in Fig. 2 where it is shown that the difference in values is maximum for  $\lambda = 0$  and decrease to zero as  $\lambda$  approaches 1. For a fixed value of  $\xi$ , the local heat flux ratio decreases as  $\lambda$  increases.

For a fixed value of  $\lambda$ , the local heat flux ratio increases quadratically for  $0 < \xi < 3$  and increases linearly when  $\xi > 3$ .

The overall surface heat flux for a cylinder with a length  $L$  can be computed from

$$Q_c = S \int_0^L q_c(x) dx \quad , \quad (53)$$

where  $S$  is the spanwise dimension which is equal to  $2\pi r_0$  for a cylinder with radius  $r_0$ . Substituting Eq. (51) into Eq. (53) and performing the integration, we have

$$Q_c = \begin{cases} S k_m A^{3/2} \sqrt{\frac{\rho_\infty g \beta K}{\mu \alpha}} \frac{L^2}{2} [-\theta'(\xi_0, 0)] \quad , & \text{for } \lambda=1 \quad , \\ S k_m A^{3/2} \left(\frac{2}{1-\lambda}\right) \sqrt{\frac{\rho_\infty g \beta K}{\mu \alpha}} \xi_L^{-\frac{(3\lambda+1)}{1-\lambda}} L^{\frac{3\lambda+1}{2}} \int_0^{\xi_L} \xi^{\frac{4\lambda}{1-\lambda}} [-\theta'(\xi, 0, \lambda)] d\xi \quad , & \text{for } \lambda \neq 1 \quad , \end{cases} \quad (54a)$$

$$\left( S k_m A^{3/2} \left(\frac{2}{1-\lambda}\right) \sqrt{\frac{\rho_\infty g \beta K}{\mu \alpha}} \xi_L^{-\frac{(3\lambda+1)}{1-\lambda}} L^{\frac{3\lambda+1}{2}} \int_0^{\xi_L} \xi^{\frac{4\lambda}{1-\lambda}} [-\theta'(\xi, 0, \lambda)] d\xi \quad , \text{ for } \lambda \neq 1 \quad , \right) \quad (54b)$$

where  $\xi_L \equiv \frac{2}{r_0} \sqrt{\frac{\mu \alpha L}{K \rho_\infty \beta g (T_w - T_\infty)_L}}$ . It is noted that the integration for  $\lambda = 1$  can be carried out explicitly since  $\xi_0$  is a constant and independent of  $x$ .

We now consider the ratio of total surface heat transfer for a vertical cylinder to that of a vertical flat plate with the same length embedded in a porous medium. The total surface heat flux for a vertical flat plate with a length  $L$  and a width  $S = 2\pi r_0$  embedded in a porous medium is given by [5]

$$Q_p = S k_m A^{3/2} \sqrt{\frac{\rho_\infty g \beta K}{\mu \alpha}} \left(\frac{2}{1+3\lambda}\right) L^{\frac{1+3\lambda}{2}} [-\theta'(0, \lambda)] \quad . \quad (55)$$

It follows that the ratio of Eqs. (54) to Eq. (55) gives

$$\left. \frac{Q_c}{Q_p} \right|_{\lambda=1} = \frac{[-\theta'(\xi_0, 0, \lambda)]_{\lambda=1}}{[-\theta'(0, \lambda)]_{\lambda=1}} \quad , \quad (56a)$$

and

$$\frac{Q_c}{Q_p} \Big|_{\lambda \neq 1} = \frac{(1+3\lambda)}{(1-\lambda)} \xi_L^{-\frac{(1+3\lambda)}{(1-\lambda)}} \int_0^{\xi_L} \frac{[-\theta'(\xi, 0, \lambda)]}{[-\theta'(0, \lambda)]} \xi^{\frac{4\lambda}{1-\lambda}} d\xi \quad (56b)$$

Numerical integration was carried out for the integral in Eq. (56b) with  $\lambda = 0, 1/4, 1/3, 1/2,$  and  $3/4$  for the range of  $\xi_L$  from 0 to 10. It is found that (1) the values of  $Q_c/Q_p$  given by Eq. (56b) is practically independent of  $\lambda$  (within 4%) for both the local similarity and the local non-similarity solution; (2) the difference in values given by the local similarity and the non-local similarity solution is within 2% as is shown in Fig. 3. Thus we may conclude from the numerical results that

$$\frac{Q_c}{Q_p} \Big|_{\text{any } \lambda} \approx \frac{[-\theta'(\xi_0, \cdot, \lambda)]_{\lambda=1}}{[-\theta'(0, \lambda)]_{\lambda=1}} \quad (57)$$

It follows that

$$Q_c \approx C S k_m A^{3/2} \sqrt{\frac{\rho_\infty g \beta K}{\mu \alpha}} \left(\frac{2}{1+3\lambda}\right)^L \frac{1+3\lambda}{2} \quad (58)$$

where the values of  $C$ , which is tabulated in Table 3, depends on  $\xi_L$  and  $\lambda$  for  $\lambda \neq 1$ , and depends on  $\xi_0$  for  $\lambda = 1$ .

#### ACKNOWLEDGMENT

This study is part of the Hawaii Geothermal Project funded in part by the RANN program of the National Science Foundation of the United States (Grant No. GI-38319), the Energy Research and Development Administration of the United States (Grant No. E(04-3)-1093), and by the State and County of Hawaii.

## REFERENCES

1. Macdonald, G.A., *Volcanoes*, Prentice-Hall, Inc., Englewood Cliffs, New Jersey, 1972.
2. White, D.C., "Characteristics of Geothermal Resources," *Geothermal Energy Resources, Production, Stimulation*, Edited by P. Kruger and C. Otte, Stanford University Press, 1973.
3. Wooding, R.A., "Convection in a Saturated Porous Medium at Large Rayleigh Number or Peclet Number," *J. Fluid Mechanics*, Vol. 15, 1963, 527-544.
4. McNabb, A., "On Convection in a Porous Medium," Proceedings of the 2nd Australasian Conference on Hydraulics and Fluid Mechanics, University of Auckland, New Zealand, C161-C171, 1965.
5. Cheng, P. and W.J. Minkowycz, "Similarity Solution for Free Convection About a Dike," Hawaii Geothermal Project Technical Report No. 10, October 28, 1975.
6. Cheng, P. and I-Dee Chang, "Buoyancy Induced Flows in a Porous Medium Adjacent to Impermeable Horizontal Surfaces," Hawaii Geothermal Project Technical Report No. 12, November 1975.
7. Sparrow, E.M. and H.S. Yu, "Local Non-Similarity Thermal Boundary Layer Solutions," *J. Heat Transfer*, Vol. 93, 1971, 328-334.
8. Minkowycz, W.J. and E.M. Sparrow, "Local Non-Similar Solutions for Natural Convective on a Vertical Cylinder," *J. Heat Transfer*, Vol. 96, 1974, 178-183.

TABLE 1 VALUES OF  $[-\theta'(\xi, \lambda, 0)]$

$\xi$	$\lambda=0$		$\lambda=1/4$		$\lambda=1/3$		$\lambda=1/2$		$\lambda=3/4$		$\lambda=1$
	LS*	LNS**	LS*	LNS**	LS*	LNS**	LS*	LNS**	LS*	LNS**	Exact
0.25	.4855	.4899	.6748	.6729	.7234	.7240	.8177	.8167	.9383	.9385	1.046
0.50	.5272	.5332	.7186	.7175	.7672	.7688	.8620	.8616	.9832	.9837	1.091
0.75	.5664	.5747	.7609	.7604	.8096	.8120	.9050	.9052	1.026	1.028	1.135
1.00	.6049	.6149	.8021	.8023	.8510	.8540	.9471	.9478	1.069	1.071	1.179
2.00	.7517	.7668	.9587	.9607	1.009	1.014	1.106	1.110	1.233	1.235	1.345
3.00	.8915	.9085	1.106	1.110	1.158	1.164	1.259	1.263	1.387	1.390	1.502
4.00	1.024	1.044	1.268	1.252	1.301	1.308	1.405	1.409	1.537	1.540	1.654
5.00	1.154	1.176	1.381	1.391	1.441	1.449	1.549	1.553	1.683	1.687	1.803
6.00	1.283	1.305	1.518	1.529	1.580	1.589	1.691	1.696	1.829	1.833	1.952
7.00	1.413	1.435	1.655	1.667	1.727	1.729	1.835	1.839	1.976	1.980	2.102
8.00	1.544	1.565	1.795	1.806	1.868	1.870	1.980	1.984	2.124	2.128	2.253
9.00	1.678	1.696	1.937	1.947	2.006	2.013	2.127	2.130	2.276	2.278	2.407
10.00	1.815	1.830	2.083	2.091	2.153	2.159	2.278	2.280	2.429	2.432	2.564

\*LS -- Local similarity solution

\*\*LNS -- Local non-similarity solution

TABLE 2 LOCAL HEAT FLUX RATIO,  $q_c(\xi)/q_p(\xi)$

$\xi$	$\lambda=0$		$\lambda=1/4$		$\lambda=1/3$		$\lambda=1/2$		$\lambda=3/4$		$\lambda=1$
	LS*	LNS**	LS*	LNS**	LS*	LNS**	LS*	LNS**	LS*	LNS**	Exact
0.00	1.000	1.000	1.000	1.000	1.000	1.000	1.000	1.000	1.000	1.000	1.000
0.50	1.183	1.202	1.140	1.140	1.132	1.132	1.125	1.125	1.101	1.101	1.090
1.00	1.362	1.386	1.271	1.272	1.257	1.258	1.241	1.242	1.200	1.200	1.178
1.50	1.531	1.561	1.399	1.400	1.371	1.372	1.350	1.351	1.294	1.294	1.262
2.00	1.696	1.727	1.520	1.522	1.486	1.488	1.450	1.452	1.383	1.384	1.343
2.50	1.853	1.889	1.637	1.641	1.597	1.601	1.549	1.552	1.469	1.470	1.420
3.00	2.005	2.044	1.753	1.759	1.707	1.712	1.648	1.652	1.554	1.556	1.496
4.00	2.304	2.351	1.976	1.986	1.919	1.927	1.840	1.845	1.721	1.723	1.649
5.00	2.601	2.645	2.192	2.205	2.123	2.133	2.030	2.036	1.887	1.890	1.801
6.00	2.894	2.941	2.411	2.429	2.330	2.342	2.221	2.227	2.053	2.056	1.951
7.00	3.189	3.236	2.631	2.650	2.538	2.551	2.410	2.417	2.218	2.221	2.102
8.00	3.481	3.530	2.851	2.870	2.747	2.760	2.602	2.609	2.385	2.389	2.254
9.00	3.771	3.821	3.071	3.090	2.953	2.967	2.791	2.799	2.551	2.555	2.406
10.00	4.060	4.110	3.289	3.309	3.159	3.173	2.981	2.989	2.721	2.725	2.561

\*LS -- Local similarity solution

\*\*LNS -- Local non-similarity solution

TABLE 3 VALUES OF  $C(\xi_L, \lambda)$  AND  $C(\xi_0)$

$\xi_L$ or $\xi_0$	$C(\xi_L, \lambda)$					$C(\xi_0)$
	$\lambda=0$	$\lambda=1/4$	$\lambda=1/3$	$\lambda=1/2$	$\lambda=3/4$	$\lambda=1$
0.0	.4440	.6303	.6788	.7615	.8926	1.000
0.5	.4840	.6900	.7400	.8300	.9729	1.090
1.0	.5230	.7425	.7996	.8970	1.051	1.178
1.5	.5603	.7954	.8566	.9610	1.126	1.262
2.0	.5962	.8464	.9116	1.023	1.199	1.343
2.5	.6305	.8950	.9639	1.081	1.267	1.420
3.0	.6642	.9429	1.015	1.139	1.335	1.496
4.0	.7322	1.039	1.119	1.256	1.472	1.649
5.0	.7996	1.135	1.223	1.371	1.608	1.801
6.0	.8662	1.230	1.324	1.486	1.741	1.951
7.0	.9333	1.325	1.427	1.601	1.876	2.102
8.0	1.001	1.421	1.530	1.716	2.012	2.254
9.0	1.068	1.517	1.633	1.832	2.148	2.406
10.0	1.137	1.614	1.738	1.950	2.286	2.561



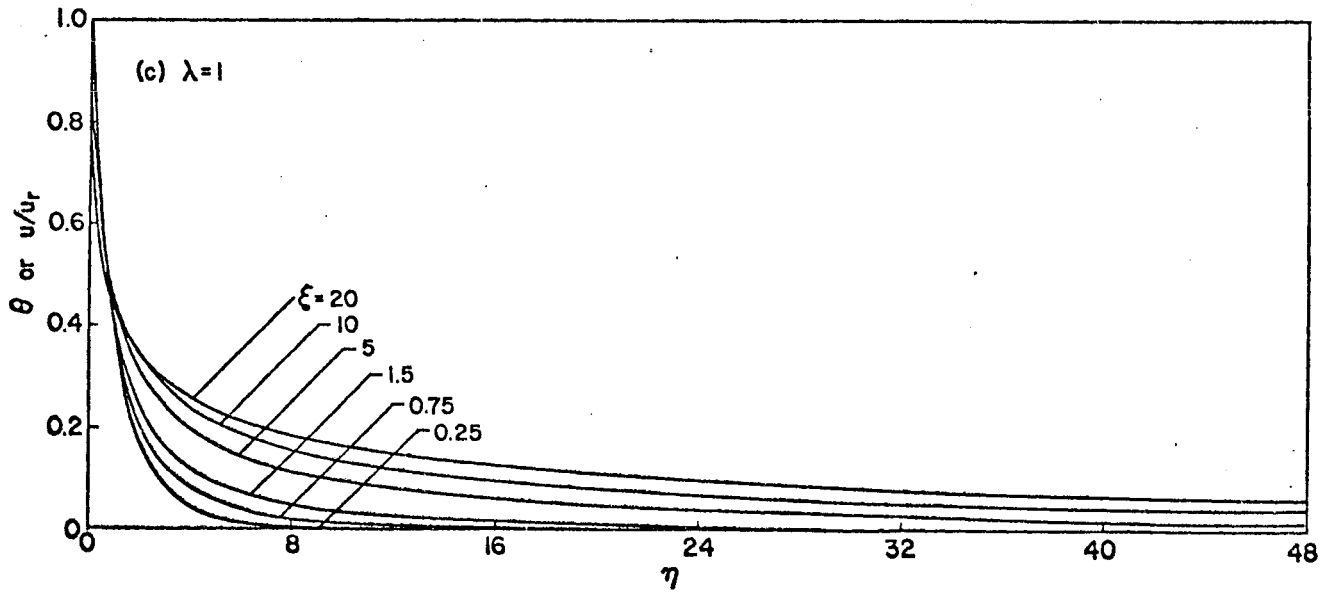
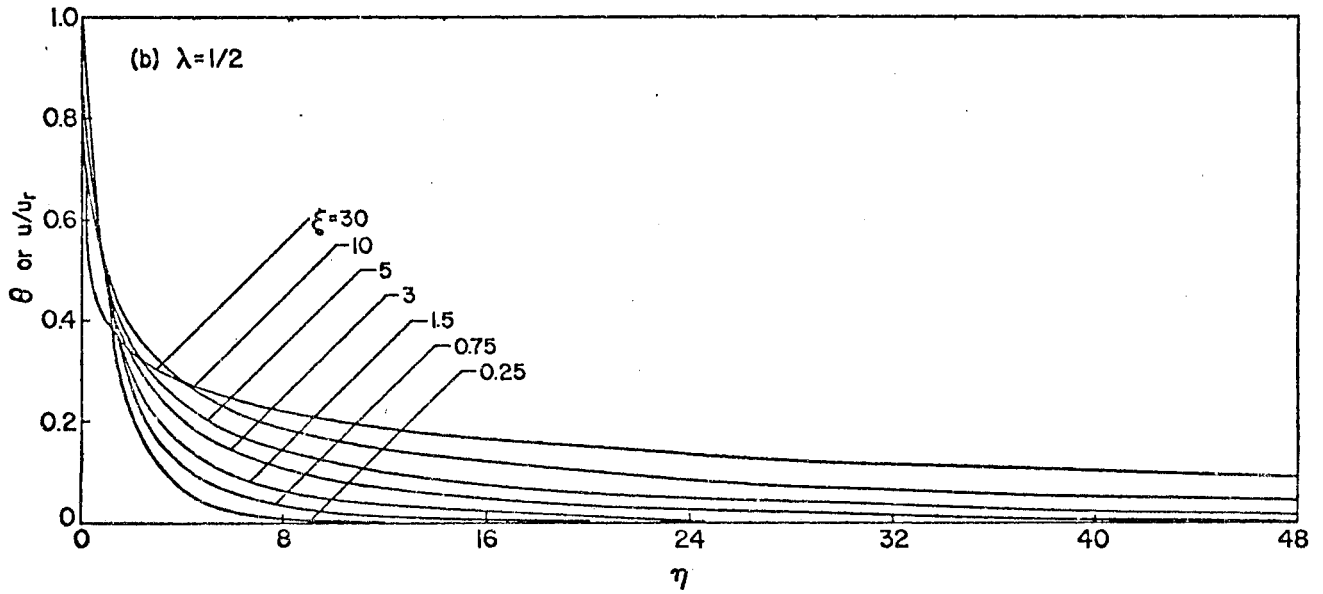
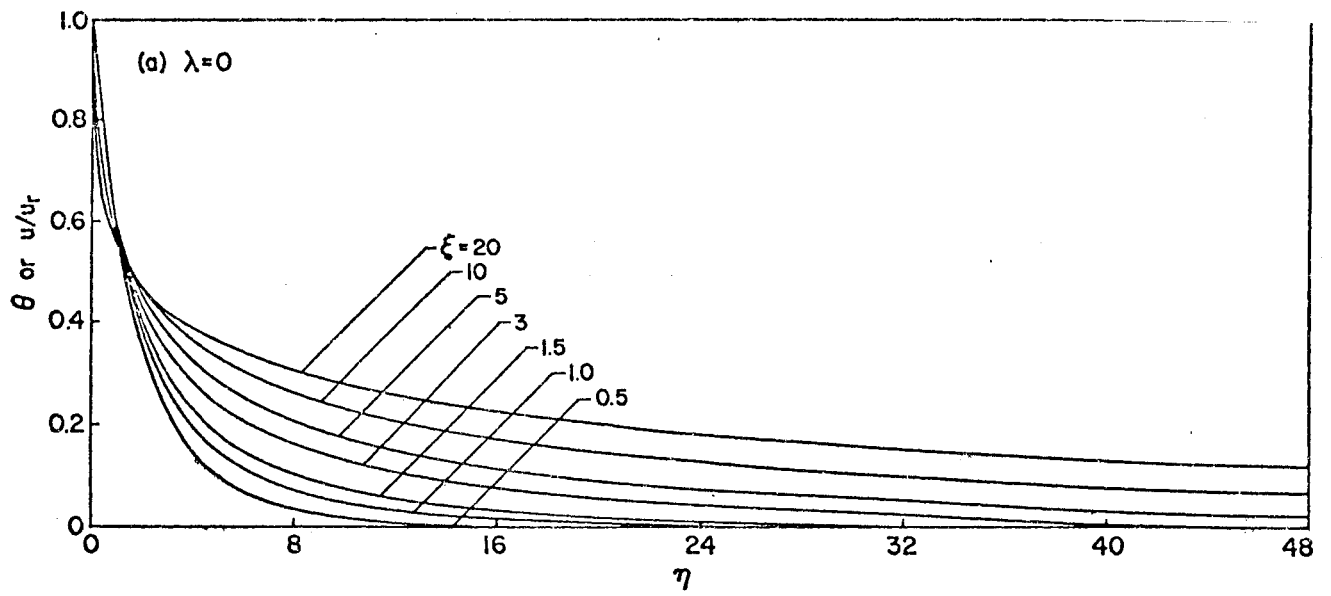


Fig. 1 DIMENSIONLESS TEMPERATURE AND VERTICAL VELOCITY PROFILES  
 (a)  $\lambda = 0$ , (b)  $\lambda = 1/2$ , (c)  $\lambda = 1$

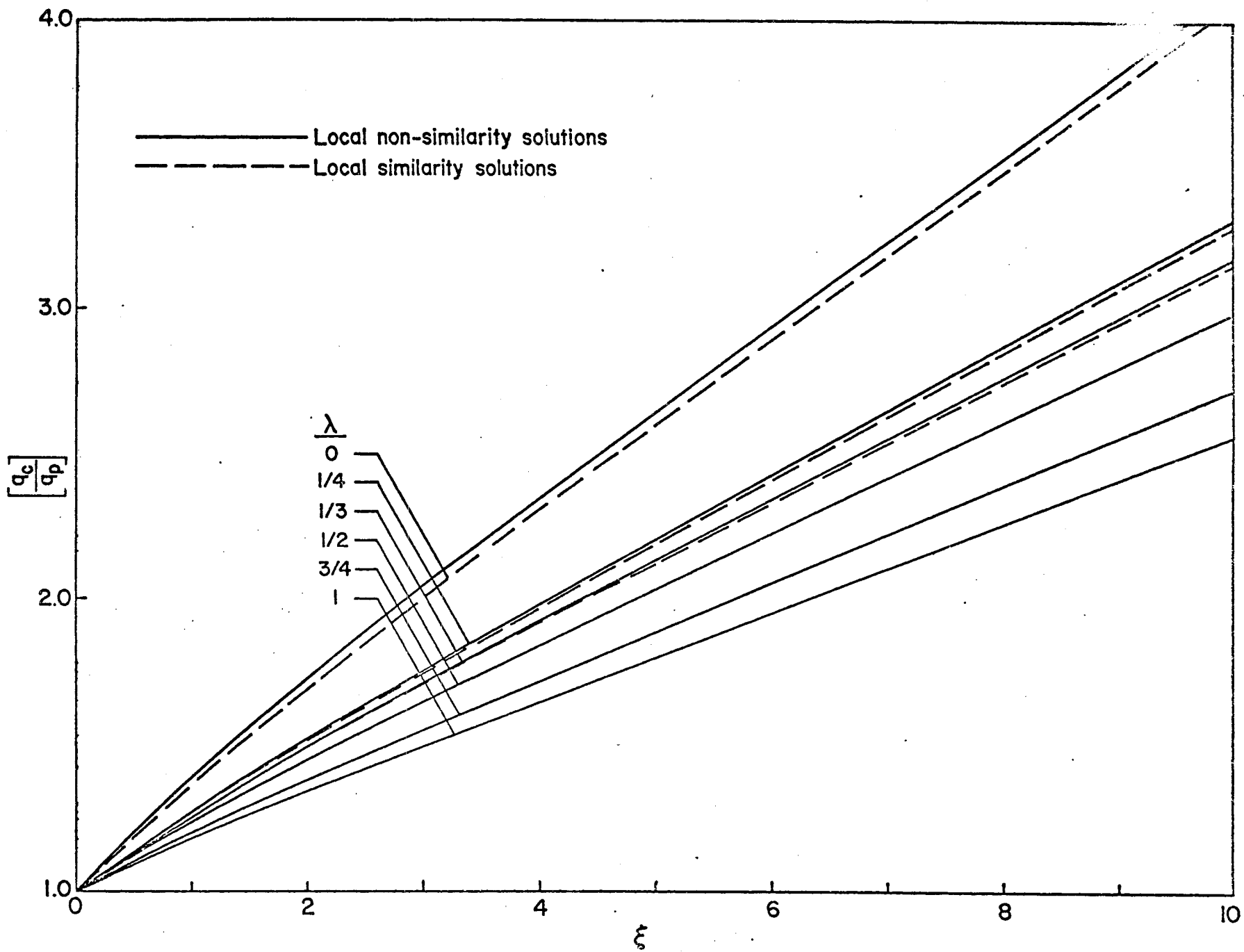


Fig. 2 LOCAL SURFACE HEAT TRANSFER RATIO FOR SELECTED VALUES OF  $\lambda$

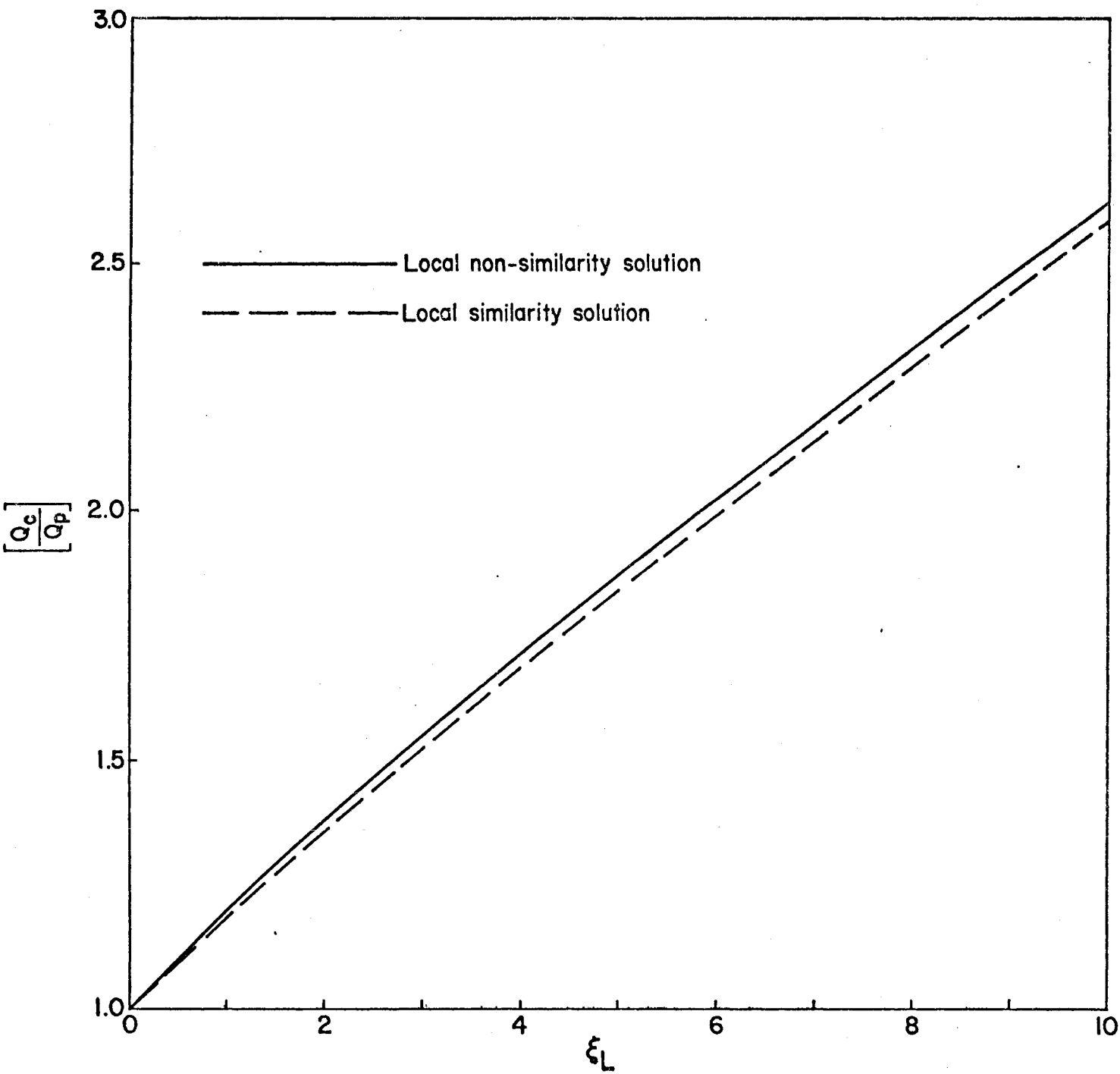


Fig. 3 TOTAL SURFACE HEAT TRANSFER RATIO FOR ANY  $\lambda$